Journal of Pharmaceutical and Biomedical Analysis 50 (2009) 655–663

Contents lists available at ScienceDirect

Journal of Pharmaceutical and Biomedical Analysis

journal homepage: www.elsevier.com/locate/jpba

# Improving the capillary electrophoretic analysis of poliovirus using a Plackett–Burman design

Iuliana Oita[a], Hadewych Halewyck[b], Sigrid Pieters[a], Bieke Dejaegher[a], Bert Thys[b], Bart Rombaut[b], Yvan Vander Heyden[a,*]

[a] Department of Analytical Chemistry and Pharmaceutical Technology, Pharmaceutical Institute, Vrije Universiteit Brussel – VUB, Laarbeeklaan 103, 1090 Brussels, Belgium
[b] Pharmaceutical Biotechnology & Molecular Biology, Vrije Universiteit Brussel – VUB, Laarbeeklaan 103, 1090 Brussels, Belgium

ARTICLE INFO

*Article history:*
Received 14 July 2008
Received in revised form
19 September 2008
Accepted 30 September 2008
Available online 10 October 2008

*Keywords:*
Poliovirus
Capillary electrophoresis
Optimization
Plackett–Burman design

ABSTRACT

Separation techniques may offer interesting alternatives to classical virological techniques both for fundamental research purposes and for vaccine manufacturing. A capillary electrophoretic method for the analysis of the poliovirus was developed based on conditions for the human rhinovirus taken from literature. The method was optimized using a 12-experiment Plackett–Burman design, applied in order to examine simultaneously the effects of eight factors on responses such as, mobility of the electroosmotic flow, effective mobility of the poliovirus, analysis time and resolution between the virus peak and a system peak. The proposed method manages to perform an acceptable separation of poliovirus particles using a 50 mM borate buffer with 25 mM SDS, in an uncoated fused-silica capillary upon application of 10 kV at 30 °C. The linearity of the proposed method was investigated for a range of poliovirus dilutions up to 140 μg/mL.



## 1. Introduction

From an extreme evolutionary point of view, virus particles can be seen as structures that evolved to transfer nucleic acids from one cell to another. To structural biology researchers, viruses represent systems which are well-defined and accessible enough to enable the investigation of the mechanistic details of assembly and maturation events or the changes in subunit structures that mediate translocation across membranes [1]. To molecular biology researchers, viruses are models for creating molecular containers that incorporate the symmetry of their capsid [2]. To separation science researchers, viruses are challenging analytes because of the colloidal nature of the virus sample, their size being several orders of magnitude larger than usual chemicals or drugs; because of their amphoteric nature, their aggregation tendency and their sensitivity to environmental changes (pH, ionic strength, solvents and surfactants) [3]. Moreover, most viral samples are also available in low volumes, highly diluted and with a matrix that interferes with most separation techniques. Unlike most chemical substances, no highly purified and highly concentrated references are available for viruses.

In modern virology, a variety of instrumental techniques are used, e.g. radioimmuno-assays, enzyme-linked immunosorbent assays, western blots, polymerase chain reaction (PCR) related techniques, most of them requiring complicated and time-consuming sample preparation and well-skilled analysts [4]. During the last 20 years, several attempts have been made to use separation techniques in virology. There is a limited number of papers reporting the use of high-performance liquid chromatographic (HPLC) techniques solely for the assessment of viral components (proteins or nucleic acids) [5–8]. Capillary electrophoresis (CE) has proven to have a great potential for the analysis of intact full viruses, subviral complexes and virus complexes [9–12]. The outer surface of viruses may be electrically charged in an aqueous environment as a result of protonation or deprotonation of amino acids residues. Under these conditions an electric double layer is developed, which creates the prerequisites for the electrophoretic mobility of the virus or sub-viral particles in an electric field. CE in the analysis of full viruses was first demonstrated in 1987 by Hjerten et al. [10]. Despite the great potential of CE in viral analysis, only a limited number of viruses have been studied [9,11,12]. Different aspects related to the human rhinovirus (HRV) have been investigated so far, such as the separation of different serotypes, the separation and biospecific identification of subviral particles, the kinetics of its thermal denaturation, and the affinities between HRVs and antibodies or receptors [13–16].

* Corresponding author. Tel.: +32 2 477 47 34; fax: +32 2 477 47 35.
*E-mail address:* yvanvdh@vub.ac.be (Y.V. Heyden).

0731-7085/$ – see front matter © 2008 Elsevier B.V. All rights reserved.
doi:10.1016/j.jpba.2008.09.049

HRV is a member of the *Picornaviridae*, one of the largest families of pathogens that comprises excellent models for the study not only of protein–protein or protein–nucleic acids interactions, but also of virus assembly [17]. Picornaviruses are small non-enveloped viruses with a capsid built up from 60 replicas of four small viral proteins (VP1, VP2, VP3, VP4) arranged on a icosahedral lattice. The capsids enclose a positive-stranded 7200–8500 nucleotide long RNA [18]. The most extensively studied member of the *Picornaviridae* is the poliovirus (PV). It is a 30 nm virus which shares most biochemical and biophysical characteristics with all *Picornaviridae*. The main differences between poliovirus and the other picornaviruses are the buoyant density in cesium chloride, the high physical and chemical stability, and the receptor binding mechanism [1,19]. Despite the impressive amount of studies on the poliovirus, not all replication steps can be fully explained or linked [20–22]. On sucrose gradient centrifugation analysis, different subviral particles (5S, 14S and 74S) can be detected during the replication cycle. These subviral particles, finally, assemble into 160S virions (the infectious particles). By exposing virions (160S particles) to elevated temperatures or extreme pH, some degradation particles can be obtained *in vitro* [23–25]. For example, heating the 160S virions at 56 °C for 20 min will result in the loss of the viral RNA (vRNA) and the capsid protein VP4. An empty capsid with a sedimentation coefficient of 80S remains [25]. There have been attempts to use a CE method in order to separate and quantify reverse transcriptase PCR products from the polio virus [26].

The similarity between HRV and PV encouraged us to test PV using similar CE separation conditions as described in Ref. [27], even though the CE method transfer is far from evident. The conditions initially applied did not result in a successful separation of the poliovirions peak from the system peak migrating with a similar velocity as the electroosmotic flow (EOF) (Rs ~0.93). The aim of this research was to develop a CE method that will provide a good separation of the poliovirions (160S) peak from that neighbouring peak in a reasonable analysis time with a good repeatability. During several preliminary experiments, the experimental domain of interest for voltage, temperature, buffer composition and sample dilution was delimitated. Afterwards, a two-level screening design was applied to identify the factors with the highest impact on the EOF and viral mobilities, the resolutions and retention factors, and, occasionally, to select optimal conditions for the separation of virions [28,29].

The proposed research is to be seen in the context of an increased regulatory pressure meant to guarantee the safety and efficiency of medicines, and also in response to the manufacturers' need to decrease the production time. Most current virological techniques provide qualitative or semi-quantitative data with poor sensitivity and limited accuracy, but employ expensive reagents, and procedures that are complicated and time-consuming. Therefore, the concepts of modern separation techniques applied to virology might solve the needs of both regulatory authorities and vaccine manufacturers.

## 2. Theory

### 2.1. Set-up of the two-levels Plackett–Burman design

Eight factors expected to have an influence on CE separation were examined at two levels in order to identify those with the greatest impact on the quality of the poliovirus separation, and/or to select optimal conditions for the separation of virions and, possibly, subviral particles [28,29]. The extreme levels of each factor (Table 1) were set based on literature [27,29,30] and experience from preliminary experiments. A 12-experiment, 11-factor Plackett–Burman design (Table 2) was selected because of the particular ability of these designs to map the experimental domain in a minimal number of experiments. To complete the 11 factors in the design, three dummy factors were added to the eight examined. The dummy effects will be used for a statistical evaluation of the factor effects [29].

**Table 1**
Factors and levels investigated in the screening design. Level '1' represents the high factor level, level '−1' the low factor level and level 0 the central level.

| Factor | Factor type | Level −1 | Level 0 | Level 1 |
|---|---|---|---|---|
| *A* | Buffer concentration (mM) | 50 | 125 | 200 |
| *B* | SDS concentration (mM) | 5 | 15 | 25 |
| *C* | Capillary temperature (°C) | 17 | 20 | 30 |
| *D* | Voltage (kV) | 10 | 20 | 30 |
| *E* | pH | 8.3 | 9.0 | 9.7 |
| *F* | Injection time to express injection volume (s) | 5 | 10 (11.26 nl) | 15 |
| *G* | Acetonitrile in BGE (%) | 0 | 5 | 10 |
| *H* | $MgCl_2$ solution added to the sample (mM) | 0[a] | 10 | 20 |

SDS = sodium dodecylsulphate; BGE = background electrolyte; $MgCl_2$ = magnesium chloride.
[a] Sample is diluted with a 24% sucrose solution.

The first aim of the design approach was to improve separation between the poliovirus and system peaks. A shorter analysis time was taken into account as a secondary goal. Initially, the following responses were considered: the electroosmotic flow mobility ($\mu_{EOF}$), the virus net effective mobility ($\mu_{eff\ virus}$), the analysis time (AT) and the resolution between the virus and system peaks (Rs).

The EOF mobility ($\mu_{EOF}$) and the apparent mobility of the virus ($\mu_{apparent\ virus}$) were calculated as follows

$$\mu_{EOF\ or\ apparent\ virus} = \frac{LL_D}{Vt_m} \quad (1)$$

where $L$ is total capillary length (m), $L_D$ the effective length (m), $V$ the applied voltage (V), and $t_m$ the migration time (s) of the EOF or the virus, respectively [30]. Virus net effective mobility ($\mu_{eff\ virus}$) was then calculated as follows [30],

$$\mu_{eff\ virus} = |\mu_{apparent\ virus} - \mu_{EOF}| \quad (2)$$

Under the applied conditions (Table 1), the poliovirus is negatively charged (pI = 7.0) [31], and so its migration tendency is directed towards the anode. The virus particles cannot compensate the dragging force of the EOF, so they move opposite to their own mobility. Thus, all 160S virions effective mobilities had a negative sign and the net effective mobility was considered.

The internal standard (IS) migration time was considered as analysis time. The migration window was calculated as the difference between the migration time of the IS and that of an EOF marker.

To quantify the quality of separation, resolution was used, calculated as follows

$$Rs = \frac{2(t_2 - t_1)}{w_2 + w_1} \quad (3)$$

where $t_2$ and $w_2$ are the migration time and baseline width of the virus peak, and $t_1$ and $w_1$ those of the system peak [32].

A composite response, $Q^*$, was defined based on Derringer's desirability functions in order to identify the most desirable conditions, i.e. with a good separation of the native poliovirus peak from the system peak in an acceptable analysis time [28,33,34]. From Eq. (2) it is obvious that a high value for the virus net mobility results from a large difference between the virus migration time and EOF time, whereas a larger migration window influences Rs indirectly,

**Table 2**
A 12-experiments Plackett–Burman design to evaluate the influences of eight experimental factors (Table 1) and three dummy factors ($d1$, $d2$, $d3$) on the responses $\mu_{EOF}$, $\mu_{eff\ virus}$, MW, AT, Rs, and $Q^*$. The responses, the estimated effects, the critical effects from dummy effects (DM) and from the algorithm of Dong (ME) are also shown.

| Exp | Factors | | | | | | | | | | | Responses | | | | |
|---|---|---|---|---|---|---|---|---|---|---|---|---|---|---|---|---|
| | *A* | *B* | *C* | *d*1 | *D* | *E* | *F* | *d*2 | *G* | *d*3 | *H* | $\mu_{EOF}$ ($10^9 \times m^2 \times V^{-1} \times s^{-1}$) | $\mu_{eff\ virus}$ ($10^9 \times m^2 \times V^{-1} \times s^{-1}$) | MW (min) | AT (min) | Rs |
| 1 | +1 | +1 | −1 | +1 | +1 | +1 | −1 | −1 | −1 | +1 | −1 | 38.02 | 0.00 | 0.00 | 3.23 | 0.00 |
| 2 | −1 | +1 | +1 | −1 | +1 | +1 | +1 | −1 | −1 | −1 | +1 | 59.96 | 0.00 | 6.73 | 8.89 | 0.00 |
| 3 | +1 | −1 | +1 | +1 | −1 | +1 | +1 | +1 | −1 | −1 | −1 | 37.94 | 0.00 | 0.00 | 9.06 | 0.00 |
| 4 | −1 | +1 | −1 | +1 | +1 | −1 | +1 | +1 | +1 | −1 | −1 | 46.25 | 1.77 | 7.44 | 10.14 | 0.00 |
| 5 | −1 | −1 | +1 | −1 | +1 | +1 | −1 | +1 | +1 | +1 | −1 | 67.94 | 7.74 | 2.45 | 4.38 | 0.99 |
| 6 | −1 | −1 | −1 | +1 | −1 | +1 | +1 | −1 | +1 | +1 | +1 | 47.53 | 0.00 | 0.00 | 7.31 | 0.00 |
| 7 | +1 | −1 | −1 | −1 | +1 | −1 | +1 | +1 | −1 | +1 | +1 | 38.33 | 0.00 | 0.00 | 3.20 | 0.00 |
| 8 | +1 | +1 | −1 | −1 | −1 | +1 | −1 | +1 | +1 | −1 | +1 | 34.73 | 0.00 | 0.00 | 9.88 | 0.00 |
| 9 | +1 | +1 | +1 | −1 | −1 | −1 | +1 | −1 | +1 | +1 | −1 | 48.46 | 7.36 | 14.02 | 21.22 | 0.97 |
| 10 | −1 | +1 | +1 | +1 | −1 | −1 | −1 | +1 | −1 | +1 | +1 | 62.71 | 9.13 | 9.31 | 14.88 | 2.42 |
| 11 | +1 | −1 | +1 | +1 | +1 | −1 | −1 | −1 | +1 | −1 | +1 | 53.46 | 5.06 | 5.15 | 7.53 | 1.20 |
| 12 | −1 | −1 | −1 | −1 | −1 | −1 | −1 | −1 | −1 | −1 | −1 | 54.32 | 5.14 | 5.33 | 11.75 | 1.86 |
| | | | | | | | | | | | | 49.14[a] | 3.02[a] | 4.20[a] | 9.29[a] | 0.62[a] |

| Responses | Effects | | | | | | | | | | | Critical effects | |
|---|---|---|---|---|---|---|---|---|---|---|---|---|---|
| | | | | | | | | | | | | $E_{critical\ DM.\ \alpha=0.05}$ | $E_{critical\ ME.\ \alpha=0.05}$ |
| $\mu_{EOF}$ | −14.63 | −1.57 | 11.88 | −2.97 | 3.04 | −2.90 | −5.45 | −2.31 | 1.18 | 2.72 | 0.63 | 8.53 | 6.44 |
| $\mu_{eff\ virus}$ | −1.89 | 0.05 | 3.73 | −0.71 | −1.18 | −3.45 | −2.99 | 0.18 | 1.28 | 2.04 | −1.30 | 3.99 | 4.59 |
| MW | −2.02 | 4.10 | 4.15 | −1.11 | −1.15 | −5.35 | 0.99 | −2.01 | 1.28 | 0.19 | −1.34 | 4.22 | 4.94 |
| AT | −0.54 | 4.17 | 3.41 | −1.19 | −6.12 | −4.33 | 1.36 | −1.39 | 1.57 | −0.51 | −1.35 | 3.50 | 5.36 |
| Rs | −0.52 | −0.11 | 0.62 | −0.03 | −0.51 | −0.91 | −0.92 | −0.10 | −0.19 | 0.22 | −0.03 | 0.45 | 0.76 |

[a] Average responses.

creating the spatial prerequisite for a high resolution. $Q^*$ was calculated as the geometric mean of the desirability coefficients for virus net mobility, migration window, and analysis time. To calculate the desirability coefficients, one-sided transformations of the measured responses were performed favouring a maximal virus net mobility and migration window and a minimal analysis time. For virus net mobility and migration window the desirability coefficients were calculated with Eq. (4), while for analysis time, Eq. (5) was used:

$$d_i = \frac{Y_i - Y^-}{Y^+ - Y^-} \tag{4}$$

$$d_i = \frac{Y^+ - Y_i}{Y^+ - Y^-} \tag{5}$$

where $d_i$ represents the desirability coefficient, $Y_i$ the measured response for experiment $i$ and $Y^-$ and $Y^+$ the smallest and largest measured responses, respectively. The combined response $Q^*$ is then calculated with Eq. (6) [28,33,34].

$$Q* = \sqrt[3]{d_{\mu_{\text{eff virus}}} \times d_{\text{MW}} \times d_{\text{AT}}} \tag{6}$$

### 2.2. Analysis of the Plackett–Burman design results

After performing the design experiments, the effect of each factor was calculated as [29],

$$E_X = \frac{\sum Y(+1) - \sum Y(-1)}{N/2} \tag{7}$$

where $E_X$ is the effect of factor $X$, $\sum Y(+1)$ and $\sum Y(-1)$ are the sums of the responses where factor $X$ is at (+1) or (−1) level, respectively, and $N$ is the number of the design experiments.

The statistical analysis of the effects was combined with a graphical interpretation using half-normal probability plots (not shown). To create and interpret half-normal probability plots, we refer to Ref. [35]. In these plots, effects are considered significant if they deviate from the straight line formed by the non-significant effects. The significance of each effect was statistically evaluated using a two-sided $t$-test [29]. To evaluate whether a given effect is significantly different from 0, the following statistic was calculated,

$$t_{\text{calc}} = \frac{|E_x|}{\text{S.E.}_{(\text{e})}} \tag{8}$$

where $\text{S.E.}_{(\text{e})}$ is the standard error of the effect. The test statistic, $t_{\text{calc}}$, is compared with a tabulated $t$-value, $t_{\text{critical}\,(\alpha,\text{d.f.})}$, with significance level $\alpha = 0.05$ and for the number of degrees of freedom (d.f.) associated with $\text{S.E.}_{(\text{e})}$. In practice, the effects were compared with a critical effect calculated by multiplying the standard error of an effect $\text{S.E.}_{(\text{e})}$ with the critical $t$-value as in Eq. (9). The critical effect is obtained from rewriting Eq. (8).

$$E_{\text{critical}} = t_{(\alpha,\text{d.f.})} \times \text{S.E.}_{(\text{e})} \tag{9}$$

To estimate the $\text{S.E.}_{(\text{e})}$ two approaches were used, i.e. one based on negligible (dummy) effects and one on the algorithm of Dong.

For the dummy factors approach, $\text{S.E.}_{(\text{e})}$ was estimated as [35],

$$\text{S.E.}_{(\text{e})} = \sqrt{\frac{\sum E_D^2}{n_D}} \tag{10}$$

where $E_D$ represents a dummy effect and $n_D$ the number of dummies. In this case d.f. equals $n_D$.

The algorithm of Dong initially estimates a standard error $s_0$, based on all effects. The final estimation, $s_1$, is made using effects considered not important based on $s_0$ [35,36]:

$$s_0 = 1.5 \times \text{median}|E_i| \tag{11}$$

$$\text{S.E.}_{(\text{e})} = s_1 = \sqrt{m^{-1} \sum E_j^2} \tag{12}$$

where $E_i$ is the effect of factor $i$, $E_j$ is an effect that, in absolute value is smaller than or equal to $2.5 \times s_0$, and $m$ the number of such effects. Here d.f. for $t_{\text{critical}}$ is $m$. For all approaches, $|E_x|$ larger or equal to $E_{\text{critical}}$ are considered significant.

The Plackett–Burman design, the responses, the estimated factors effects and the critical effects obtained by both statistical approaches are presented in Table 2.

### 2.3. Linearity study

The first step in the assessment of linearity consists in plotting the calibration data. A straight-line model ($y = b_0 + b_1 x$) was applied using the ratio between the peak areas of the poliovirus and of IS as $y$. Plotting the individual data revealed that the standard deviations of the signal depended on the sample concentrations $x$ (heteroscedastic data). The uniformity of variances was also verified applying a Cochran test [28]:

$$C = \frac{s_{\text{max}}^2}{\sum_j s_j^2} \tag{13}$$

where $s_{\text{max}}^2$ is the highest variance and $s_j^2$ the variance for the $j$th concentration. The $C$ value is compared with a tabulated $C$-value for $k$, $n_j$ and $\alpha$ significance level, where $\alpha = 0.05$, $k$ the number of concentrations, and $n_j$ the number of measurements at a concentration level. If $C < C_{\text{tabulated}}$, the data are considered homoscedastic.

Since data were found to be heteroscedastic, the calibration line was calculated by weighted least squares (WLS) regression [28]. A goodness-of-fit test was used to verify whether the calibration curve is best fitted by a straight line rather than by a second degree model [28].

## 3. Materials and methods

### 3.1. Chemicals and reagents

All chemicals were used without further purification. Sodium dodecyl sulphate (SDS, 98.5%) was purchased from Sigma (Steinheim, Germany) and *o*-phtalic acid (*puriss*, >99.5%) from Fluka (Steinheim, Germany). Methanol HPLC grade, acetonitrile HPLC grade and sodium hydroxide 1 M were from Fisher Scientific (Leicestershire, UK). Acetone was from VWR International (Leuven, Belgium). All other chemicals were purchased from Merck (Darmstadt, Germany).

Ribonuclease A solution (from bovine pancreas, 50% solution in glycerol, 29 mg/mL) and Proteinase K (2360 U/mg), both from Sigma–Aldrich (Saint-Louis, MO, USA), were used for initial investigations. RNase ONE (Ribonuclease 10 U/μL) from Promega Corporation (Madison, WI USA) and Proteinase K (20 mg/mL, nuclease free, sterile, double distilled water, Roche Diagnostics, Penzberg, Germany) were used for virus peak investigations after the experimental design.

PV RNA was synthesised *in vitro* by transcription of poliovirus genome from full length clones of pT7PVM using a Ribomax Large Scale RNA Production System T7 (Promega Corporation) as described earlier [37]. PV RNA, at a concentration of about 260 ng/μL, was collected in RNase-free water, obtained using a Nanopure Diamond water purification system (Barnstead, Dubuque, Iowa, USA).

### 3.2. Solutions

All solutions were prepared using Milli-Q water produced in-house by a Milli-Q Water Purification System (Millipore, Milford, MA, USA).

Buffers were prepared by dissolving the necessary amounts of boric acid and sodium dodecyl sulphate (SDS) in water and adjusting the pH using 1 M NaOH before bringing to volume. Any other buffer additive was added before the pH adjustment. The pH measurements were performed using a pH-meter Orion 520 A (Orion Research, Boston, MA, USA). Solutions were degassed by ultrasonication for 20 min in an ultrasonic bath (Branson Ultrasonic Corporation, CT, USA) and filtered through a polypropylene membrane with 0.2-μm pore size (VWR, Leuven, Belgium) prior to CE analysis.

### 3.3. Instrumentation

CE experiments were performed using a Beckman P/ACE MDQ CE system (Fullerton, CA), controlled by the Beckman 32 Karat software (2001 Beckman Coulter) and equipped with a diode array detector (190–600 nm). Untreated fused-silica capillaries with an inner diameter of 50 μm were purchased from Composite Metal Services (Ilkley, UK). The separation capillaries had a total length of 50.2 cm (effective length was 40 cm) and were thermostated using liquid cooling. Samples were introduced by applying a pressure of 0.7 psi to the inlet vial for a prescribed time. UV-absorption was recorded at 205, 240, 260 and 280 nm with the detector placed at the cathodic side of the capillary. The wavelengths selected were based on classical virological techniques used to assess concentration and purity of a viral preparation [4].

New capillaries were conditioned by flushing with 100 mM hydrochloric acid, followed by water, 1 M sodium hydroxide (NaOH), and water for 10 min, each time using a 20 psi pressure. Prior to each measurement the capillary was rinsed with 0.1 M NaOH, water, and background electrolyte (BGE) for 2 min each by applying a 14 psi pressure. If different buffers were used during the same sequence of experiments, a rinse step was performed between the two different buffers. This step comprised in flushing the capillary with water followed by 1 M NaOH, water, 0.1 M NaOH, water for 5 min each time and, finally with the specified BGE during 15 min.

Tests were performed in triplicate.

### 3.4. Samples

Poliovirus Sabin strain (type 1) was grown, collected and purified by sucrose gradient ultracentrifugation as described in [38]. The concentration of the virus in the tested sample was determined spectrophotometrically and was found to be ~5 μg/100 μL, assuming $A_{260\ nm}$ = 81.6 for a 10 mg/mL solution [39].

Virus samples used for the experimental design were diluted using a 4:1 virus:diluent ratio with the following diluents, i.e. 24% sucrose in water (diluent A), and 10 mM or 20 mM magnesium chloride prepared in diluent A.

To all samples, *o*-phtalic acid was added at a 20 μg/mL level as internal standard (IS).

The conversion of 160S virions into 80S empty capsids was done as follows: 50 μL of 160S particles was kept for 20 min at 56 °C on a water bath Ecotemp TW12 (Julabo Labortechnik, Seelbach, Germany) and then cooled on an ice bath [25].

For the enzyme treatment of the virus sample either 1 μL of RNase was added to 50 μL of sample and incubated for 15 min at 37 °C, or 0.5 μL of Proteinase K was added to 50 μL of sample and incubated for 45 min at 45 °C.

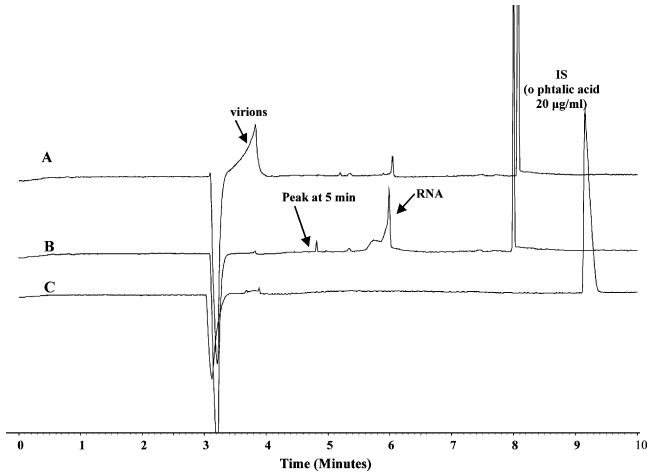


**Fig. 1.** CE separation of unheated poliovirions sample (A), heated poliovirions sample (B) and sucrose blank (C). Virus concentration ~5 μg/100 μL. Separation conditions: uncoated fused silica capillary (50.2 cm × 50 μm); 100 mM borate buffer pH 8.3 with 10 mM SDS; hydrodynamic injection at 0.7 psi for 9 s; separation voltage, 20.1 kV; temperature, 20 °C; detection wavelength 205 nm.

## 4. Results and discussions

### 4.1. Preliminary experiments

Viral samples were analyzed undiluted using the CE separation conditions for HRV described in Ref. [27]. On the electropherogram (Fig. 1, trace A) three main peaks were revealed, i.e. a big negative peak containing matrix structures that absorb only below 200 nm, followed by a peak with an absorption maximum in the 248–262 nm range and further the internal standard peak.

An indirect strategy was applied for peak identity confirmation to surmount the unavailability of reference materials. During three approaches, either the disappearance or the increase of a particular peak was monitored: (i) heat denaturation of virions, (ii) enzymatic treatment of both native virions and heat denaturated virus, (iii) RNA spiking of both native virions and heat denaturated virus.

Injecting a heated poliovirus sample (80S empty capsids), the peak at 3.8 min disappeared and two other appeared, at about 5.0 and 5.8 min, respectively (trace B on Fig. 1). The peak detected around 5.8 min is absorbing with maximum intensity in the 250–270 nm range, indicating it might correspond to RNA. If samples incubated with RNase or proteinase K were injected, the peak at 3.8 min was still revealed on the electropherograms (unpublished results). Upon injecton of 80S empty capsids or 160S virions, spiked with vRNA, a visible increase was noticed in the peak migrating around 5.8 min (Fig. 2). Therefore the peak at 3.8 min was assigned to the poliovirions and that at 5.8 min to vRNA.

Three sucrose concentration levels (20%, 25%, and 30%, respectively) prepared in phosphate buffer saline (PBS) pH 7.4 were tested during a matrix investigation. Two rationales were behind these tests: literature reports on chargeable complexes formed between sugars and borate buffers at alkaline pH [40], and identification of the source of the negative peak. The composition of the matrix blank was set taking into account the last purification step of the viral sample—a differential centrifugation and rate zonal density sedimentation in a 15–30% sucrose gradient prepared in PBS and poliovirus buoyant density. The matrix proved responsible for the negative peak, but not for other peaks present on viral samples electropherograms.

As the background electrolyte (BGE) can be considered a ternary mixture of two anions (borate and dodecylsulphate) and the sodium cation, a theoretical evaluation using the freeware

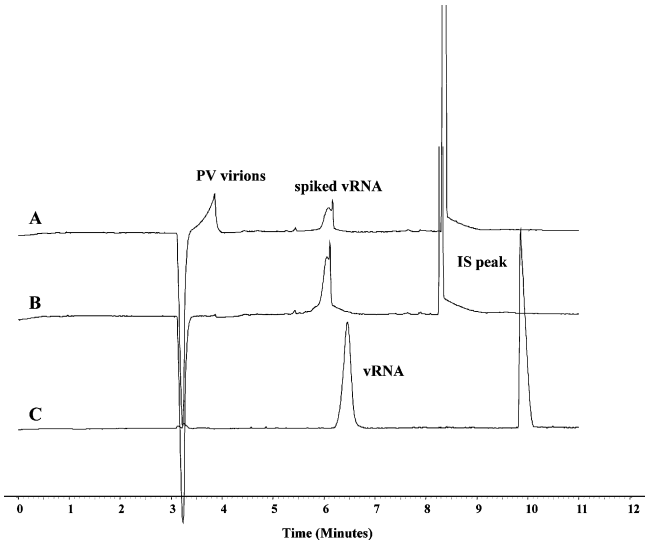


**Fig. 2.** CE separation of samples spiked with vRNA: (A) 33 μL 160S native poliovirions spiked with 260 ng vRNA, (B) 33 μL heated poliovirus (80S) spiked with 260 ng vRNA, (C) 130 ng/μL RNA in water. Separation conditions as in Fig. 1.

Peakmaster 5.2 [41] indicates three possible system zones [41–44]. The first has zero mobility and represents the water gap or the injection zone and can be used as an EOF marker. The second is moving with a mobility of $0.006 \times 10^9\ m^2 \times V^{-1} \times s^{-1}$, while the third has an anionic mobility of $-24 \times 10^9\ m^2 \times V^{-1} \times s^{-1}$. Sucrose, the major component of the virus sample, is entrapped between the first two system zones since it does not possess any ionisable groups and hence no electrophoretic mobility of its own. Moreover, sucrose does not possess any chromophores, hence it exhibits no UV or visible light absorption, generating a negative signal when passing the detector. The proximity of the poliovirus peak to the system peak leads to a two-way interaction responsible for the enlargement and the dispersion of both peaks due to a resonance phenomenon [42–44]. A complementary source for peak broadening and distortions comes from the colloidal nature of the virus sample, responsible for an electrophoretic heterogeneity due to a wide distribution of charges, size, and shapes [12].

In the initial conditions, an analysis time of 8.1 min was obtained. The peak attributed to the poliovirus had a migration time of ~3.8 min and a net electrophoretic mobility of $\sim 9.75 \times 10^9\ m^2 \times V^{-1} \times s^{-1}$, consistent with the published data for other picornaviruses [13].

A 60 s difference (~13% of migration window) between the EOF and the virus zones was recorded, which is not enough to ensure a proper resolution between the viral peak and the system peak (Rs ~0.92). The EOF is more than five times higher than the net virus mobility, thus separation conditions that decrease the EOF velocity (i.e. adding organic additives to the buffer, reducing electrical field intensity, increasing buffer concentration) may be favouring Rs [45].

Several factors such as voltage, temperature, injection time and buffer composition also are known to have an influence on electrophoretic separation [28,29]. During a series of experiments, preliminary attempts were made to identify those factors most influencing the mobility of EOF, the virus effective mobility, and the resolutions in order to evaluate them more thoroughly later in an experimental design.

To evaluate the effect of a voltage increase, 20, 25 and 29 kV were applied at 20 °C, using three buffers: 50 mM borate containing 25 mM SDS, 100 mM borate containing 10 mM SDS and 200 mM borate containing 10 mM SDS. The concentration of SDS was increased for the 50 mM borate buffer to limit the analyte-wall interactions. While the mobility of the EOF showed little variation irrespective of the level of voltage employed, the virus mobility showed an obvious increase when 25 kV was applied. The broadening of the virus peak was higher in case of the 29 kV, indicating a possible excessive Joule heating in the sample zone, due to the high salt content of the sample matrix (data not shown). Further experiments performed at 10 kV gave sharper virus peaks.

Temperature is expected to increase mobilities and decrease the analysis time at the expense of separation quality [30]. Surprisingly, keeping other separation conditions constant, a 10 °C increase in temperature did not increase the virus mobility compared to the initial values, but produced a slight increase in EOF mobility. In the case of 200 mM borate buffer with 10 mM SDS, both mobilities were about 20% lower compared to the initial levels. None of the tested conditions improved the resolution between the poliovirus and neighbouring peak.

Brij 35 and sodium deoxycholate were tested as alternatives to SDS, for which a disintegration action against poliovirus 80 S empty capsids is indicated in the literature [46]. Only a slight improvement of the resolution was recorded when Brij 35 was used, and no improvement for the sodium deoxycholate compared to the initial conditions.

Three different solvents, i.e. acetone, methanol and acetonitrile, were tested at three levels as buffer selectivity adjusters. The highest level investigated was set at 10% to avoid unnecessary destabilization in the running buffer micellary system [47]. Buffers containing acetone caused a negative shift in absorbance. Both methanol and acetonitrile decreased the EOF and virus mobility. Resolution between the poliovirus and the matrix peaks was not significantly improved, while an increase in efficiency was noticed. Buffers containing acetonitrile resulted in a larger migration window and narrow peaks. Hence acetonitrile addition to the BGE was considered for further investigations.

The tested viral sample has a complex matrix containing both non-ionic and ionic components. This limits a stacking approach and explains the peak broadening and low plate numbers [48]. To compensate the matrix effect, viral samples were diluted with either a 100 or 10 mM borate buffer without SDS, or with magnesium chloride solutions. A 4:1 ratio of virus:diluent was used to avoid an excessive dilution of the viral sample. To exclude false positive results due to the effect of dilution on the viscosity of the samples, virus samples diluted with a 24% sucrose solution were used as reference. The addition of magnesium chloride to the viral sample seemed to slightly increase the resolution. Hence sample dilution with $MgCl_2$ was considered for further investigations.

### 4.2. Screening design

From the above preliminary experiments, it was not obvious which factors had the greatest influence on the separation. Moreover, several other factors not tested during the preliminary experiments might exert an influence on the separation quality. Therefore, eight factors, i.e. buffer concentration, surfactant concentration, temperature, voltage, pH, injection volume, percent of organic modifier in the buffer, and inorganic additive added to the sample, were selected to be screened using a two-level 12-experiment Plackett–Burman design (Tables 1 and 2) [28,29].

Samples were examined using the experimental conditions specified by the experimental design. It was impossible to perform the design within 1 day. Therefore, at the beginning and end of each working day an experiment was performed at central factor levels. The responses were plotted as a function of time in order

**Table 3**
Derringer desirability values for the considers responses. For each experiment $Q^*$ was calculated as the geometric mean of the desirability values.

| Experiment no | Derringer desirability values for the considered responses | | | $Q^*$ |
|---|---|---|---|---|
| | $\mu_{\text{eff virus}}$ | MW | AT | |
| 1 | 0.00 | 0.00 | 1.00 | 0.00 |
| 2 | 0.00 | 0.48 | 0.68 | 0.00 |
| 3 | 0.00 | 0.00 | 0.67 | 0.00 |
| 4 | 0.19 | 0.53 | 0.61 | 0.40 |
| 5 | 0.85 | 0.17 | 0.93 | 0.52 |
| 6 | 0.00 | 0.00 | 0.77 | 0.00 |
| 7 | 0.00 | 0.00 | 1.00 | 0.00 |
| 8 | 0.00 | 0.00 | 0.63 | 0.00 |
| 9 | 0.81 | 1.00 | 0.00 | 0.00 |
| 10 | 1.00 | 0.66 | 0.35 | 0.62 |
| 11 | 0.55 | 0.37 | 0.76 | 0.54 |
| 12 | 0.56 | 0.38 | 0.53 | 0.48 |

MW = migration window; AT = analysis time.

to detect possible drifts. No drift in the responses was found (data not shown), and thus no correction of the responses prior to effect estimation was needed [49].

Based on the statistical approaches, two factors were considered to have a significant effect on $\mu_{\text{EOF}}$, i.e. borate concentration ($A$) and capillary temperature ($C$) (Table 2). Higher buffer concentrations decrease the Zeta-potential of both the capillary wall (for generating EOF) and the virus, they may increase peak efficiency speeding up the analysis time, but will also increase the current, generating more heat. The temperature is known to decrease the viscosity with 2% for each 1 °C temperature increase [30]. Consequently ion mobility will be increased.

On $\mu_{\text{eff virus}}$ none of the factors were found to be significant. The effects of factors $C$ (capillary temperature), $E$ (pH) and $F$ (injection volume) were found to be the largest anyway.

The analysis time is significantly decreased by the voltage ($D$) and the pH ($E$) and increased by the SDS concentration ($B$). Capillary temperature ($C$) was found to have a borderline significant direct effect. The statistical approach revealed two clearly significant factors on Rs, i.e. $F$ (injection time) and $E$ (pH). Factors $A$ (borate concentration), $C$ (capillary temperature), and $D$ (voltage) were found to have smaller significant effects. In literature, a fast reduction of plate number and separation is reported as the sample volume is increased [50]. These might be consequences of overloading, as the sample plug becomes longer than the dispersion caused by the analyte diffusion. Also, in this case, an increased sample plug will intensify the perturbations in BGE concentration favouring baseline disturbances. At higher pH, the EOF is increased and the ionization of negatively chargeable groups at the viral surface is promoted, discouraging the interactions between the virus particle and SDS monomers/micelles.

Resolution is improved at higher temperatures ($C$) due to improved column efficiency and also probably due to a significant increase of $\mu_{\text{EOF}}$ and $\mu_{\text{eff virus}}$. Since the temperature effect on $\mu_{\text{EOF}}$ is almost three times that of $\mu_{\text{eff virus}}$, a reasonable difference in mobilities will be induced and therefore Rs will increase. Increased voltage ($D$) proved to have a significant negative effect on resolution, altering both selectivity and efficiency of separation.

The borate concentration ($A$) was found to have a negative influence on Rs, although literature data point to the beneficial influence of a BGE concentration increase on resolution [30]. For six design experiments no separation was seen and Rs was defined as 0. A closer look at the experimental conditions revealed that for five of these experiments at least one of the main unfavourable factors from an Rs point of view, i.e. pH ($E$) and injection volume ($F$), was at the high level. The experimental conditions were also at high level for the buffer concentration in experiments 1, 3, 6, 7, 8. For the sixth experiment without separation (experiment 2) the buffer concentration is at a low level but both other are at a high level. The above is reflected in the effects of these three factors on the Rs (Table 2).

Moreover, the comparative analysis of the analytical conditions of "good" versus "bad" experiments for the different responses was rather inconclusive. This led us to the definition of a combined response, $Q^*$, a reflection of the main objectives of the study, i.e. obtaining a good resolution in an acceptable time. A value of 0 for $Q^*$ reflects a set of undesirable experimental conditions since they do not satisfy the objectives. Only five experiments had a "desirability" value different from 0, i.e. experiments 10, 11, 5, 12, 4 (in descending order of $Q^*$) (Table 3 and Fig. 3). Four of these experiments were

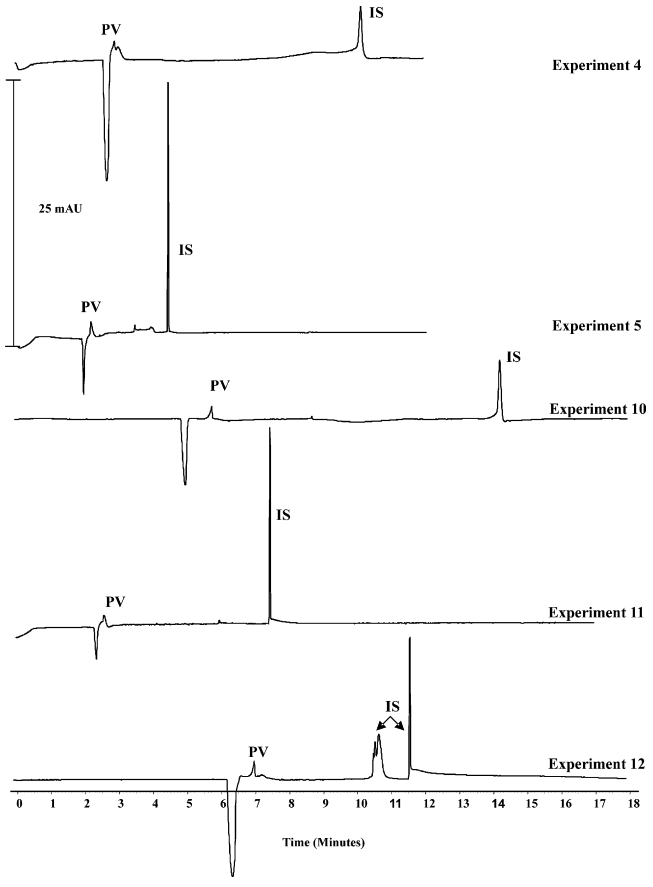


**Fig. 3.** CE separation of unheated poliovirions (PV) (A). Experiments with $Q^* > 0$. Virus concentration ~5 μg/100 μL. Uncoated fused silica capillary (50.2 cm × 50 μm). Detection wavelength at 205 nm. Experimental conditions as in Table 2.

**Table 4**
Average response of the PV calibration line, variances for each concentration level ($n = 3$), the outputs of Cocran's test and lack of fit test.

| | Dilution level | | | | | | | Cochran's test | | Lack of fit | |
|---|---|---|---|---|---|---|---|---|---|---|---|
| | 100% | 85% | 70% | 55% | 40% | 25% | 10% | $C_{calculated}$ | $C_{0.05,7,3}$ | $F$ | $P$-Value |
| Response (PV peak area/IS peak area) | 0.48 | 0.38 | 0.28 | 0.20 | 0.14 | 0.075 | 0.019 | 0.672 | 0.230 | 0.14 | 0.72 |
| Variance | 0.021 | 0.008 | 0.00087 | 0.00060 | 0.0004 | 0.000036 | 0.000015 | | | | |

performed at the low levels of borate concentration, pH and injection volume. The most desirable experiment, (experiment 10, Fig. 4) showed an improved separation of the virus peak from the matrix peak ($Q^* = 0.62$) somewhat at the expense of analysis time. Both resolution (from 0.93 to 2.42) and efficiency (from 6500 to 38700 theoretical plates) were noticeably increased compared to the initial experiments. The relative standard deviation (R.S.D.) calculated for virus migration time was 0.38% for six replicates (1 day).

### 4.3. Further investigations using the most desirable conditions

The conditions from the most desirable experiment were used to re-confirm the peak identities, to check the linearity of the method and the ability to separate subviral particles. The experiments were performed using a poliovirus sample with a 14 μg/100 μL concentration.

The same strategy as in discussed higher was applied for peak identity confirmation. The peak of the poliovirus (160S virions) is shown in Fig. 4 (trace A). After heating, the 160S virions peak disappeared completely and a new trio of peaks (trace B peaks 1–3) appeared in the 12–14 min time range. These peaks might be from to 80S empty capsids, vRNA, and clusters of viral proteins. The first peak from this trio has an absorption maximum at 260 nm, the second absorbs with maximum intensity in the low UV range (190–210 nm) and the last both in the low UV range and at 240 and 280 nm. To identify these three peaks, several attempts are being considered, i.e., spiking with vRNA, and enzyme incubation, but further research is still required to investigate in more detail (Halewyck et al., in preparation).

The linearity of the relationship between peak area and the concentration of the viral sample was assessed by injecting seven dilutions of the poliovirus sample. The undiluted sample at a 14 μg/100 μL concentration was considered as 100%. Further dilutions were expressed as % from the initial sample concentration, maintaining a constant sample volume. The dilutions were equally distributed in 10–100% range, i.e. 10–25–40–55–70–85–100%. Samples were diluted using a 24% sucrose solution in 5 mM borate buffer to avoid variation due to viscosity changes. For the 10% dilution, the signal-to-noise ratio for the virus peak was about 10, close to the limit of quantification according to the ICH guidelines [51]. Three independent experiments were performed, at each concentration level.

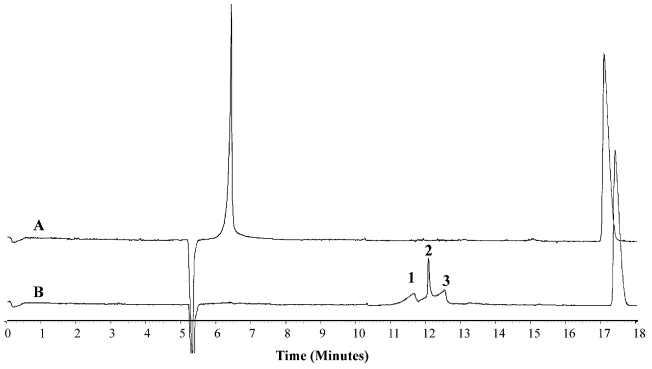


**Fig. 4.** CE separation of unheated poliovirions (A) and heated poliovirions (B). Virus concentration ~14 μg/100 μL. Conditions: uncoated fused silica capillary (50.2 cm × 50 μm); 50 mM borate buffer pH 8.3 with 25 mM SDS; hydrodynamic injection at 0.7 psi for 5 s; separation voltage 10 kV; cartridge temperature 30 °C; detection wavelength 205 nm.

The average responses (PV peak area divided by IS peak area) for all dilutions are given in Table 4. Visual inspection of the plotted data (responses versus concentration) revealed a higher variability of the responses for the higher concentration levels, which was confirmed by a Cochran test. Ordinary least square regression (OLS) resulted in a residual plot where residuals are not randomly distributed, due to the data heteroscedasticity. Therefore, a weighted least squares (WLS) was necessary. This resulted in a residual plot without an obvious tendency (data not shown). The calibration line, obtained using WLS, showed linearity for the investigated range as demonstrated by the lack of fit test (Table 4). The following equation was found: $y = -0.684 + 0.0133 \pm 0.0055x$, at a 95% confidence interval. The linear relationship between PV area and concentration encourages us to see this method as an alternative to current methods for PV quantification in poliomyelitis vaccines [52].

## 5. Conclusions and future perspectives

A simple capillary electrophoresis method was developed and optimized. The proposed method manages to perform an acceptable determination of poliovirus particles using a 50 mM borate buffer, pH 8.3 containing 25 mM sodium dodecylsulphate, in an uncoated fused-silica capillary (50 μm i.d., total length 50.2 cm, effective length 40 cm) upon application of 10 kV at 30 °C.

A linear calibration curve can be used for quantitative experiments, but the heteroscedaticity needs to be taken into account and WLS should be applied for modelling. The method was also applicable on heated samples, but more investigations should be done on the ability of separating subviral particles. Further, signal improvement using intra-column mechanisms will be tested in order to obtain fast reliable results with a minimal sample preparation and an increased sensitivity.

The above method is fast and inexpensive, and therefore represents an interesting alternative to current tests used to assay PV concentration during manufacturing and for batch release of inactivated polio vaccine.

## Acknowledgements

Bieke Dejaegher is a postdoctoral Fellow of the Research Foundation – Flanders (FWO). This work was supported by a Horizontale Onderzoeksactie (HOA) of the Vrije Universiteit Brussel and a research grant (G.0051.08) of the FWO-Vlaanderen. We thank Monique De Pelsmacker for the preparation of the viruses, and Katrien Decq and Frank Van der Kelen for the technical and logistic assistance.

## References

[1] A.C. Oliveira, D. Ishimaru, R.B. Gonçalves, T.J. Smith, P. Mason, D. Sá-Carvalho, J.L. Silva, Biophys. J. 76 (1999) 1270–1279.
[2] A.J. Olson, Y.H.E. Hu, E. Keinan, Proc. Natl. Acad. Sci. U.S.A. 104 (2007) 20731–20736.
[3] M.J. Desai, D.W. Armstrong, Microbiol. Mol. Biol. Rev. 67 (2003) 38–51.

[4] B.W.J. Mahy, H.O. Kangro (Eds.), Virology Methods Manual, Academic Press, London, 1996.
[5] D. Chelius, A.F.R. Huhmer, C.H. Shieh, E. Lehmberg, J.A. Traina, T.K. Slattery, E. Pungor, J. Proteome Res. 1 (2002) 501–513.
[6] E. Takahashi, S.L. Cohen, P.K. Tsai, J.A. Sweeney, Anal. Biochem. 349 (2006) 208–217.
[7] V. Garcia-Canas, B. Lorbetskie, D. Bertrand, T.D. Cyr, M. Girard, Anal. Chem. 79 (2007) 3164–3172.
[8] A. Foriers, B. Rombaut, A. Boeyé, J. Chromatogr. 498 (1990) 105–111.
[9] L. Kremser, G. Bilek, D. Blaas, E. Kenndler, J. Sep. Sci. 30 (2007) 1704–1713.
[10] S. Hjerten, K. Elenbring, F. Kilar, J.L. Liao, A.J.C. Chen, C.J. Siebert, M.D. Zhu, J. Chromatogr. 403 (1987) 47–61.
[11] E. Kenndler, D. Blaas, Trends Anal. Chem. 10 (2001) 543–551.
[12] M.A. Rodriguez, D.W. Armstrong, J. Chromatogr. B 800 (2004) 7–25.
[13] V. Okun, B. Ronacher, D. Blaas, E. Kenndler, Anal. Chem. 72 (2000) 2553–2558.
[14] V.M. Okun, D. Blaas, E. Kenndler, Anal. Chem. 71 (1999) 4480–4485.
[15] V.M. Okun, S. Nizet, D. Blaas, E. Kenndler, Electrophoresis 23 (2002) 896–902.
[16] V.M. Okun, R. Moser, D. Blaas, E. Kenndler, Anal. Chem. 73 (2001) 3900–3906.
[17] M.G. Rossmann, J.E. Johnson, Annu. Rev. Biochem. 58 (1989) 533–573.
[18] R.R. Rueckert, in: B.N. Fields, D.M. Knipe, P.M. Howley (Eds.), Fields Virology, third ed., Lippincott-Williams & Wilkins, Philadelphia, 1996, pp. 609–654.
[19] M.S. Chapman, M.G. Rossmann, Virology 195 (1993) 745–756.
[20] A. Boeye, B. Rombaut, in: J.L. Melnick (Ed.), Progress in Medical Virology, vol. 39, Karger, Basel, 1992, pp. 139–166.
[21] C.U.T. Hellen, E. Wimmer, Virology 187 (1992) 391–397.
[22] J.R. Putnak, B.A. Phillips, Microbiol. Rev. 45 (1981) 287–315.
[23] B. Rombaut, R. Vrijsen, P. Brioen, A. Boeyé, Virology 122 (1982) 215–218.
[24] B. Rombaut, R. Vrijsen, A. Boeyé, Virology 177 (1990) 411–414.
[25] F. Koch, G. Koch, The Molecular Biology of Poliovirus, Springer, Wien, 1985.
[26] E.F. Rossomando, L. White, K.J. Ulfelder, J. Chromatogr. B 656 (1994) 159–168.
[27] V.M. Okun, B. Ronacher, D. Blaas, E. Kenndler, Anal. Chem. 71 (1999) 2028–2032.
[28] D.L. Massart, B.G.M. Vandeginste, L.M.C. Buydens, S. De Jong, P.J. Lewi, J. Smeyers-Verbeke, Handbook of Chemometrics and Qualimetrics, Part A, Elsevier, Amsterdam, 1997.
[29] Y. Vander Heyden, C. Perrin, D.L. Massart, in: K. Valko (Ed.), Separation Methods in Drug Synthesis and Purification, Handbook of Analytical Separations, vol. 1, Elsevier, Amsterdam, 2000, pp. 163–212.
[30] C.F. Poole, The Essence of Chromatography, Elsevier, Amsterdam, 2003, pp. 620–706.
[31] C.P. Gerba, Adv. Appl. Microbiol. 30 (1984) 133–168.
[32] United States Pharmacopeial Convention, United States Pharmacopeia, 28th ed., United States Pharmacopeial Convention, Rockville, 2004.
[33] G. Derringer, R. Suich, J. Qual. Technol. 12 (1980) 214–219.
[34] M. Jimidar, B. Bourguignon, D.L. Massart, J. Chromatogr. A 740 (1996) 109–117.
[35] Y. Vander Heyden, A. Nijhuis, J. Smeyers-Verbeke, B.G.M. Vandeginste, D.L. Massart, J. Pharm. Biomed. Anal. 24 (2001) 723–753.
[36] F. Dong, Stat. Sin. 3 (1993) 209–217.
[37] S. Van Der Werf, J. Bradley, E. Wimmer, F.W. Studier, J.J. Dunn, Proc Natl. Acad. Sci. U.S.A. 83 (1986) 2330–2334.
[38] B. Rombaut, R. Vrijsen, A. Boeyé, J. Gen. Virol. 66 (1985) 303–307.
[39] J. Charney, R. Machlowitz, A.A. Tytell, J.F. Sagin, D.S. Spicer, Virology 15 (1961) 269–280.
[40] Z. El Rassi, Y.S. Mechef, in: Patrick Camilleri (Ed.), Capillary Electrophoresis Theory and Practice, second ed., CRC Press, Boca Ranton, 1997, pp. 273–313.
[41] PeakMaster 5.2, www.natur.cuni.cz/gas (accessed August 2008).
[42] B. Gas, V. Hruska, M. Dittmann, F. Bek, K. Witt, J. Sep. Sci. 30 (2007) 1435–1445.
[43] B. Gaš, E. Kenndler, Electrophoresis 21 (2000) 3888–3897.
[44] B. Gaš, E. Kenndler, Electrophoresis 25 (2004) 3901–3912.
[45] C. Schwer, E. Kenndler, Chromatographia 33 (1992) 331–335.
[46] L. Kremser, M. Petsch, D. Blaas, E. Kenndler, Electrophoresis 27 (2006) 1112–1121.
[47] E. Fuguet, C. Ràfols, E. Bosch, M. Rosés, Electrophoresis 23 (2002) 56–66.
[48] J. Boden, K. Bachmann, L. Kotz, L. Fabry, S. Pahlke, J. Chromatogr. A 734 (1996) 319–330.
[49] Y. Vander Heyden, A. Bourgeois, D.L. Massart, Anal. Chim. Acta 347 (1997) 369–384.
[50] Z.K. Shihabi, L. Garcia, in: J.P. Landers (Ed.), Handbook of Capillary Electrophoresis, CRC Press, Boca Raton, 1994, pp. 537–548.
[51] Guidelines prepared within the International Conference on Harmonisation of Technical Requirements for the Registration of Pharmaceuticals for Human Use (ICH), Validation of Analytical Procedures: Text and Methodology, Q2(R1), 2005, 1–13, http://www.ich.org/ (accessed August 2008).
[52] World Health Organisation, Requirements for Poliomyelitis Vaccine (Oral), WHO Expert Committee on Biological Standardization, Geneva, 1983.